The influence of fabry-perot tunable filter on dynamic strain sensing system

Author/Contributor:
Peng, Gang-Ding

Publication details:
Photonics Asia 2007: Sensors and Imaging

Event details:
Photonics Asia 2007: Sensors and Imaging
Beijing, China

Publication Date:
2007

Publisher DOI:
http://dx.doi.org/10.1117/12.756654

The Influence of Fabry-Perot Tunable Filter on Dynamic Strain Sensing System*

Liu Kun[1**], Jing Wencai[1,2***], Liu Tiegen[1], Zhang Yimo[1],
Jia Dagong[1], Zhang Hongxia[1], Peng Gangding[2]

1 College of Precision Instrument & Opto-electronics Engineering,
Tianjin University, Tianjin 300072, P. R. China,
Key Laboratory of Opto-electronics Information and Technical Science (Tianjin University),
Ministry of Education, Tianjin 300072, China
2 School of Electrical Engineering and Telecommunications, UNSW, Australia

ABSTRACT

One of the key issues in establishing an optical fiber sensing system based on fiber Bragg gratings (FBGs) is the selection of a suitable wavelength shift detection scheme in terms of the performance it offers. By use of a compact Fabry-Perot (F-P) tunable filter, the Bragg wavelength variation can be detected with a relatively high speed and satisfying resolution. In this paper, a dynamic strain sensing system based on F-P tunable filter is described, and the F-P tunable filter is demonstrated to have a significant impact on the system. The relationship between the collected spectrum of grating and the 3-dB bandwidth of the F-P tunable filter is discussed. The optimum 3-dB bandwidth of the F-P tunable filter for most FBGs is obtained. It is exhibited in this paper that the demodulation precision and sensitivity of the strain sensing system is influenced by the nonlinearity between the transmission wavelength of the F-P tunable filter and the drive voltage. The drive voltage is rectified using interpolation algorithm. The experimental results illustrate that the average error and the maximum error of the transmission wavelength are decreased by 96.4% and 80.9% respectively. The strain sensitivity of the optimized system is below $3\mu\varepsilon$. The error between the practical strain value demodulated by the system and theoretical value is below 5%.

Key words: fiber sensing, dynamic strain sensing, demodulation, Fabry-Perot tunable filter, nonlinear

1. INTRODUCTION

Fiber Bragg gratings (FBGs) have successfully been developed for use in optical fiber communication and sensing fields since 1989[1]. One of the key issues in establishing an optical fiber sensing system based on FBGs is the selection of a suitable wavelength shift detection scheme in terms of the performance it offers[2]. Several interrogation systems have been proposed. Kersey *et al* proposed a method for detecting the wavelength shift of a fiber Bragg grating utilizing an

* This work was supported by the National Natural Science Fund of China under contact No. 60577013, and the New Century Support Program for Talented Young Teachers in Universities, MOE (Ministry of Education), China

** Liu Kun: telephone number: (+86)22-27403147 , E-mail: beiyangkl@tju.edu.cn

*** Jing Wencai is now a visiting professor at UNSW, Australia

Advanced Sensor Systems and Applications III, edited by Yun-Jiang Rao, Yanbiao Liao,
Gang-Ding Peng, Proc. of SPIE Vol. 6830, 68301K, (2007)
0277-786X/07/$18 · doi: 10.1117/12.756654

unbalanced fiber interferometer[3]. Melle *et al* proposed a simple demodulation system in which the Bragg wavelength is determined from the signal ratio by dividing it using an operational amplifier[4,5]. Kersey *et al* proposed a scheme for detecting the wavelength shift of a fiber Bragg grating sensor or network of sensor elements along a common fiber path using a fiber Fabry-Perot filter[6]. Xu *et al* proposed a technique for the interrogation of in-fiber Bragg grating sensors using an acousto-optic tunable filter[7]. Davis *et al* proposed a wavelength detection scheme based on the use of a wavelength division coupler designed to exhibit a monotonic dependence of the splitting ratio on wavelength[8]. Davis *et al* proposed an all-fiber Fourier transform spectrometer for decoding the wavelength shifts from a series of Bragg grating sensors[9]. Lobo Ribeiro *et al* proposed a passive self-referencing all-fiber technique for Bragg wavelength shift detection using a biconical fiber filter[10]. Romero *et al* proposed a fiber Bragg grating interrogation technique utilizing the edge filtering concept applied to a chirped fiber Bragg grating written in an erbium-doped fiber[11].

With the use of a compact, electronically tunable fiber pigtailed Fabry-Perot (F-P) tunable filter, the Bragg wavelength variation can be detected with a relatively high speed and satisfying resolution[2], which is suitable for several different applications. So this method is widely used for interrogating the wavelength shift of FBGs in fiber sensing sytem[2,6,12,13]. However, little research on the influence of F-P tunable filter in the fiber sensing system has been performed. In this paper, a dynamic strain sensing system based on F-P tunable filter is described. Based on discussing the relationship between the collected spectrum of grating and the 3-dB bandwidth of the F-P tunable filter, the optimum 3-dB bandwidth of the F-P tunable filter for most FBGs is obtained. The nonlinearity between the transmission wavelength of the F-P tunable filter and the drive voltage is exhibited, which can be rectified using interpolation algorithm. Dynamic strain sensing can be realized using this system.

2. STRUCTURE OF DYNAMIC STRAIN SENSING SYSTEM

The schematic diagram in figure 1 shows the basic configuration of the dynamic strain sensing system based on F-P tunable filter. This system consists of broadband source, isolator and coupler, FBG array, F-P tunable filter, photodetector and LabVIEW card based on computer. The broadband source is a readily available 1555 nm single-mode pigtailed super luminescent diode (SLD, SLD 76-HP) with about 5 mW output over a 51.2 nm spectral width. The F-P tunable filter (FFP-TF2) is a compact, electronically tunable fiber pigtailed Fabry-Perot interferometric tunable filter. The cavity spacing can be tuned by an external voltage signal, which induces the transmission spectrum of the F-P tunable filter to be tuned accordingly. The free spectral range (FSR) and the bandwidth of the F-P tunable filter were measured to be 90 nm and 15 pm respectively. The photodetector is a fiber pigtailed high-speed InGaAs PIN with a $1G\Omega$ transimpedance amplifier. Several FBGs are placed along a fiber path, whose nominal Bragg wavelengths and operational wavelength domains are chosen not to overlap, and all of them fall within the spectral envelop of the broadband source. Furthermore, the FSR of the F-P tunable filter is required to be greater than the total wavelength domain occupied by FBGs.

Light from the broadband source is divided by coupler, reflected by the FBG array, and then detected by photodetector after transmission through the F-P tunable filter. The isolator is placed in the system to ensure unidirectional light in the beam of the broadband source and prevent feedback into the broadband source. The drive voltage signal of F-P tunable filter is generated from the digital-to-analogue converter (DAC) on the LabVIEW card and amplified by the low-pass amplifier before applying on the F-P tunable filter. The output signals of the photodetector are sampled using the analogue-to-digital converter (ADC) on the LabVIEW card. The DAC and ADC on the LabVIEW

card use the same sample clock to achieve synchronization, which ensures that the transmission spectrum position of the F-P tunable filter and the optical power detected by the photodetector are corresponding one by one. All of the signals are stored and analyzed by computer.

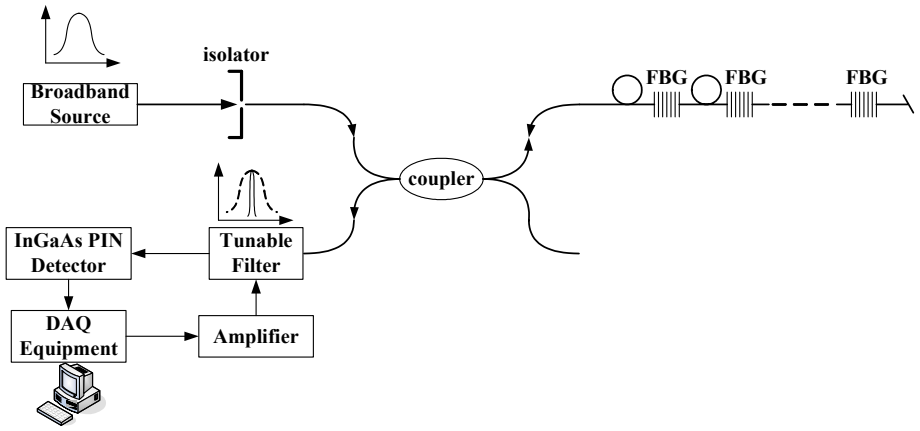

Figure 1. The schematic diagram of the dynamic strain sensing system based on F-P tunable filter

3. SELECTION OF F-P TUNABLE FILTER

The two most important parameters of the F-P tunable filter are FSR and 3-dB bandwidth. As described in Section 2, the FSR of the F-P tunable filter should be more than the spectral bandwidth of the broadband source. Thus the quantity of the FBGs is only restricted by the spectral envelop of the broadband source. In the dynamic strain sensing system, the spectral width of SLD is 51.2 nm. So the FSR of the F-P tunable filter should be more than this value. It was set to be 90 nm.

The optical spectrum analysis method was used to calculate the optimum 3-dB bandwidth of the F-P tunable filter. The FBG and the F-P tunable filter can be treated as spectral transfer functions in this method. In figure 1, the power spectrum of the broadband source is $S(\lambda)$, where λ is the wavelength. For the sake of simplicity, the reflective spectrum of the FBG and the transmitted spectrum of the F-P tunable filter can both be assumed to take a Gaussian form[13]:

$$G_{jR}(\lambda) = R_{jG} \exp\left(-\frac{4\ln 2(\lambda - \lambda_{jG})^2}{\sigma_{jG}^2} \right) \tag{1}$$

$$F_j(\lambda) = T_{jF} \exp\left(-\frac{4\ln 2(\lambda - \lambda_{jF})^2}{\sigma_{jF}^2} \right) \tag{2}$$

where $G_{jR}(\lambda)$ and $F_j(\lambda)$ are the spectral transfer function of the FBG in the reflective mode and of the F-P tunable filter respectively, R_{jG} and T_{jF} are the peak reflectivity of the FBG and the peak transmitivity of the F-P tunable filter respectively, λ_{jG} and λ_{jF} are the Bragg wavelength of the FBG and the transmission wavelength of the F-P tunable filter respectively, σ_{jG} and σ_{jF} are the spectral width of the FBG reflective spectrum and of F-P tunable filter transmitted spectrum respectively. Let ρ to be the ratio of σ_{jF} and σ_{jG},

$$\sigma_{jF} = \rho\sigma_{jG} = \rho\sigma \tag{3}$$

where σ is also to be treated as the spectral width of the FBG reflective spectrum for simplicity. $S(\lambda)$ is assumed as a constant in the reflective spectrum of FBG and the transmitted spectrum of F-P tunable filter, because its bandwidth is much larger than the others'. S is assumed as a unit light source of the power spectrum of the source. The optical power detected by photodetector can be calculated as

$$\begin{aligned} I &= \int_{-\infty}^{\infty} \frac{1}{4} * S(\lambda) * G_{jR}(\lambda) * F_j(\lambda) d\lambda \\ &= \int_{\lambda_{jF}-\rho\sigma/2}^{\lambda_{jF}+\rho\sigma/2} \frac{1}{4} * S * G_{jR}(\lambda) * F_j(\lambda) d\lambda \\ &= \frac{1}{4} SR_{iG}T_{iF}\left(\frac{\sqrt{\pi}\rho\sigma}{2\sqrt{4\ln 2}\sqrt{1+\rho^2}}\right) * \exp\left(-\frac{4\ln 2(\lambda_{jG}-\lambda_{jF})^2}{(1+\rho^2)\sigma^2}\right) * erf\left(\frac{\sqrt{4\ln 2}\left[(\lambda-\lambda_{jF})+\rho^2(\lambda-\lambda_{jG})\right]}{\rho\sqrt{1+\rho^2}\sigma}\right)\Bigg|_{\lambda_{jF}-\rho\sigma/2}^{\lambda_{jF}+\rho\sigma/2} \\ &= \frac{1}{4} SR_{iG}T_{iF}\left(\frac{\sqrt{\pi}\rho\sigma}{2\sqrt{4\ln 2}\sqrt{1+\rho^2}}\right) * \exp\left(-\frac{4\ln 2(\lambda_{jF}-\lambda_{jG})^2}{(1+\rho^2)\sigma^2}\right) \\ &\quad * \left[erf\left(\frac{\sqrt{4\ln 2}\left[\rho\sigma/2+\rho^2(\lambda_{jF}-\lambda_{jG}+\rho\sigma/2)\right]}{\rho\sqrt{1+\rho^2}\sigma}\right) - erf\left(\frac{\sqrt{4\ln 2}\left[-\rho\sigma/2+\rho^2(\lambda_{jF}-\lambda_{jG}-\rho\sigma/2)\right]}{\rho\sqrt{1+\rho^2}\sigma}\right)\right] \end{aligned} \tag{4}$$

where S, R_{jG} and T_{jF} are constant, $1/4$ is the fraction of the optical power of the broadband source at the photodetector, the error function, *erf*, is a distribution function from a normal distribution. From equation (4), it is obvious that the original bandwidth of the FBG is expanded by $\sqrt{1+\rho^2}$. In the other hand, the optical power detected by photodetector is also influenced by the difference between λ_{jG} and λ_{jF}. Therefore, the ratio ρ of σ_{jF} and σ_{jG} ($\rho = \sigma_{jF}/\sigma_{jG}$) together with the difference $\Delta\lambda$ between λ_{jG} and λ_{jF} ($\Delta\lambda = |\lambda_{iG} - \lambda_{iF}|$) are two important factors for selection of F-P tunable filter. According to equation (4), the optical power detected by photodetector is the function of ρ and $\Delta\lambda$.

When the ratio ρ is a constant, the unitary optical power detected by photodetector is the function of the difference between the central wavelength of FBG and F-P tunable filter. The figure 2 shows the relationship between them. For a special value of ρ, when the Bragg wavelength of FBG is superposed with the transmission wavelength of F-P tunable filter, the maximum optical power can be obtained. When the difference between the central wavelength of FBG and F-P tunable filter increases, the optical power decreases symmetrically. Thus, the spectrum of FBG can be collected when the transmission wavelength of F-P tunable filter is scanned through the wavelength range of FBG. This figure also exhibits that the 3-dB bandwidth of FBG is expanded by function of ρ. The 3-dB bandwidth of FBG becomes smaller with the decrease of ρ. When ρ becomes less than 0.1, the collected spectrum of FBG scarcely changes. And then it can be equal to the practical spectrum of FBG.

When the difference $\Delta\lambda$ is a constant, the optical power detected by photodetector is the function of the 3-dB bandwidth ratio of FBG and F-P tunable filter. The figure 3 shows the relationship between them. For a special value of $\Delta\lambda$, when the 3-dB bandwidth ratio between FBG and F-P tunable filter is increased, the detected optical power becomes larger. But when the ratio is larger than a value, e.g. 3 for $\Delta\lambda = 0$, the detected optical power will approach a constant and increase very slowly. And when the 3-dB bandwidth ratio between FBG and F-P tunable filter is reduced less than a value, e.g. 1 for $\Delta\lambda = 0$, the detected optical power will decrease sharply. When the ratio ρ is set to be 0.1,

the peak detected optical power will be 26dB loss of the broadband source output. If the ratio ρ is too small, the detected optical power will have too low signal noise ratio (SNR).

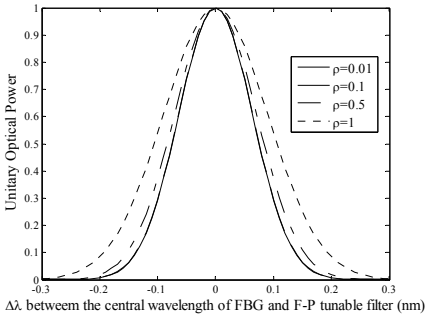

Figure 2. The relationship between the unitary optical power detected by photodetector and the central wavelength difference of FBG and F-P tunable filter

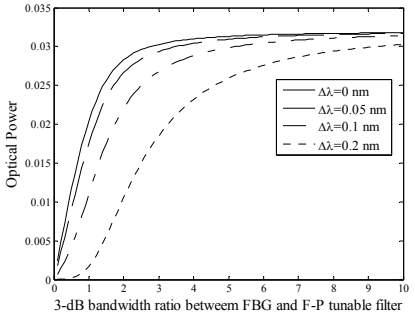

Figure 3. The relationship between the optical power detected by photodetector and the 3-dB bandwidth ratio of FBG and F-P tunable filter

The two important items described above are in contradiction with each other for choosing the ratio ρ. It is shown in figure 2 that the ratio ρ should be small. The smaller the ratio ρ is, the narrower the 3-dB bandwidth of collected spectrum is. And it is good for obtaining the peak wavelength of FBG. But in other hand, it is shown in figure 3 that the ratio ρ should be large. The larger the ratio ρ is, the better SNR is. And it is good for obtaining the spectrum of FBG. So it is crucial to find a tradeoff between them. From the analysis above, it is obvious that the optimum ratio ρ should be set to be 0.1. Additionally, the typical 3-dB bandwidth of most FBGs is 150pm[1]. So the optimum 3-dB bandwidth of the F-P tunable filter for the dynamic strain sensing system is 15pm.

4. CALIBRATION OF F-P TUNABLE FILTER NONLINEARITY

The relationship between the transmission wavelength of the F-P tunable filter and its drive voltage is nonlinear when driven by a piezoelectric actuator due to the intrinsic nonlinearity between the displacement and voltage of the actuator. Both the transmission wavelength and FSR of F-P tunable filter are nonlinear with the drive voltage. The majority of the published data on commercial piezoelectric ceramics assumes a linear relationship between the dielectric displacement and the electric field, or chooses to use only part of the FSR of the F-P tunable filter to meet the linear response

assumption if obvious nonlinearity does exit[2].

The nonlinear relationship between the transmission wavelength of the F-P tunable filter and drive voltage can be measured using tunable laser (HP8164 lightwave measurement system from Agilent Corporation) with 1 pm resolution. When the drive voltage was varied linearly from 0V to 18V, the relationship between them was shown in figure 4. Under two-order polynomial fit, the relationship between them was defined as followed

$$\lambda_T = -0.048U^2 - 4.800U + 1627.332 \tag{5}$$

where λ_T is the transmission wavelength of the F-P tunable filter, U is the drive voltage. If it were assumed as linearity, there would be too much error beyond several nanometers.

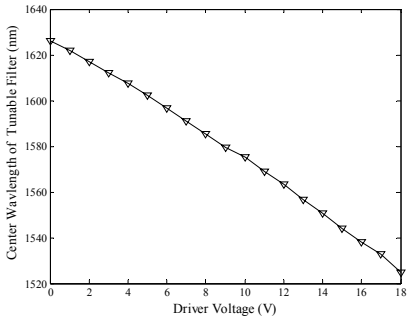

Figure 4. Relationship between the transmission wavelength of F-P tunable filter and drive voltage

The rectified drive voltage of the F-P tunable filter was obtained using interpolating algorithm. Using linear fit, the relationship between the experiment data of drive voltage and F-P tunable filter transmission wavelength was calculated as followed

$$\lambda_i = \lambda(v_i) \tag{6}$$

where $\lambda_i \in \{\lambda_0, \lambda_1, \cdots \lambda_{k-1}\}$ was the transmission wavelength of F-P tunable filter, $v_i \in \{v_0, v_1, \cdots v_{k-1}\}$ was the corresponding drive voltage, and $\lambda(\bullet)$ was a linear function which is the aim to be obtained. On the fitting curve described by equation (5), a set of wavelength $\lambda_i' \in \{\lambda_0', \lambda_1', \cdots \lambda_{k-1}'\}$ was selected to be nearest to λ_i, and the corresponding drive voltage was calculated to be $v_i' \in \{v_0', v_1', \cdots v_{k-1}'\}$ using equation (5). The rectified drive voltage list of the F-P tunable filter was obtained using the spline interpolation algorithm and $\{v_i'\}$. By use of this interpolation algorithm, the rectified drive voltage list of the F-P tunable filter between 7.2V and 18V was calculated.

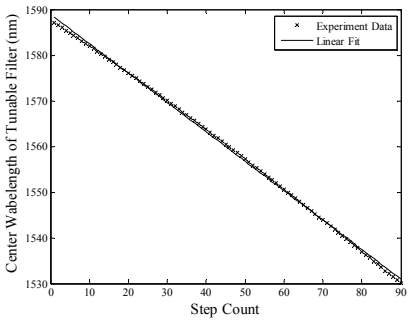

Figure 5. Transmission wavelength of the F-P tunable filter before rectification

The relationship between the transmission wavelength of the F-P tunable filter and the drive voltage with or without

rectification were both measured using tunable laser. The transmission wavelength of the F-P tunable filter when driven by the voltage without rectification was shown in figure 5. Under linear fit, the average error and the maximum error are 0.250 and 1.201 respectively. The transmission wavelength of the F-P tunable filter when driven by the voltage with rectification was shown in figure 6. Under linear fit, the average error and the maximum error are 0.009 and 0.229 respectively. By use of the interpolation algorithm, the average error and the maximum error of the transmission wavelength are decreased by 96.4% and 80.9% respectively. And the average error is below 10 pm. This is very significant for spectroscopy and wavelength interrogation.

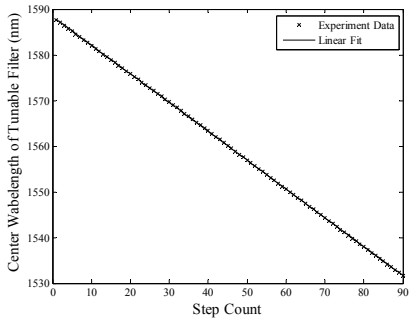

Figure 6. Transmission wavelength of the F-P tunable filter after rectification

5. DYNAMIC STRAIN SENSING EXPERIMENT

The dynamic strain sensing system based on F-P tunable filter described in figure 1 was used to realize dynamic strain sensing. Four FBGs were placed along a single-mode fiber, whose Bragg wavelengths were between 1540 nm and 1560 nm without overlapping. The spectrum of them collected by the system was shown in Figure 7. One of them was assumed to be the reference FBG, which was used to eliminate noise and error in the system. And to eliminate the influence by haphazard error, moving averaging algorithm was used to analyze the experiment data. Eight data points were used to calculate one strain value in this algorithm. And when the new point was collected, one of the eight points was replaced by the new one, and the practical strain value was updated.

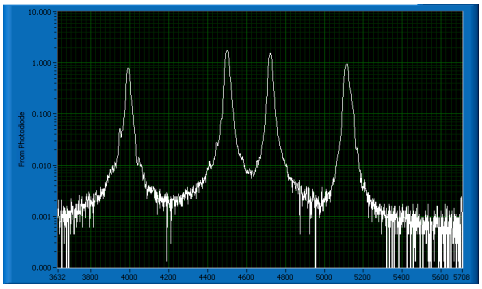

Figure 7. Spectrum of gratings collected by dynamic strain sensing system

Using moving averaging algorithm and reference FBG, the demodulation strain values of the other three FBGs were obtained. When all of them were in free state, average strain values for 800 measurements were shown in Table 1. The deviations of strain values were below $3\mu\varepsilon$. So the strain sensing sensitivity of this system was blow $3\mu\varepsilon$.

The stress on the FBGs was exhibited by the strain values demodulated using this system. When the stress was

increased, the relationship between stress and demodulation strain was shown in figure 8(a). When the stress was decreased, the relationship between stress and demodulation strain was shown in figure 8(b). Under linear fit, the slopes of figure 8(a) and figure 8(b) were $-0.0161\mu\varepsilon/g$ and $-0.0135\mu\varepsilon/g$ respectively. The latter was less than the former because of the strain remaining in FBGs when stress was decreased.

Table 1. Demodulation strain of FBGs without stress ($\mu\varepsilon$)

	FBG1	FBG2	FBG3
Deviation	2.3	2.0	2.7

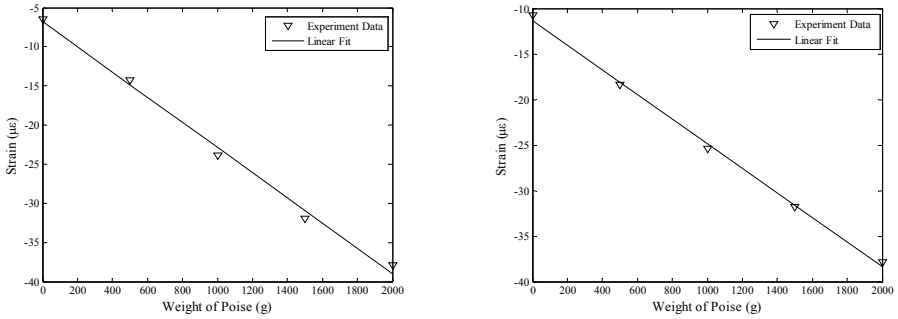

(a) stress increased (b) stress decreased

Figure 8. Relationship between demodulated strain and weight of poise

In the other hand, according to elasticity mechanics theory, strain can be calculated as followed

$$E_p \times \Delta\varepsilon = \frac{F}{S} \tag{7}$$

where $\Delta\varepsilon$ is the strain value , F is the stress , S is the effective area of stress , E_p is Young' s modulus。In this experiment, the maximum of stress was $F = 2 \times 9.8N$, the effective area of stress was $S = 2.4 \times 10^{-6} m^2$, and Young' s modulus was $E_p = 2.06 \times 10^{11} P_a$. So the maximum of theoretical strain value was $39.6\mu\varepsilon$. And the maximum of practical strain value detected using the system was $37.9\mu\varepsilon$. The error between the practical strain value demodulated by the system and theoretical value was below 5%.

6. CONCLUSION

A dynamic strain sensing system based on F-P tunable filter is described in this paper. And the F-P tunable filter is demonstrated to have a significant impact on the system. The relationship between the collected spectrum of grating and the 3-dB bandwidth of the F-P tunable filter is discussed. The relationship between the detected optical power and the 3-dB bandwidth of the F-P tunable filter is also discussed. And as a result of discussion, the optimum 3-dB bandwidth of the F-P tunable filter for most FBGs is 15 pm. It is exhibited the nonlinearity between the transmission wavelength of the F-P tunable filter and the drive voltage in this paper. The drive voltage is rectified using interpolation algorithm. The experimental results illustrate that the average error and the maximum error of the transmission wavelength are decreased by 96.4% and 80.9% respectively. The average error is below 10 pm after drive voltage rectification. Dynamic strain sensing can be realized using this system. The strain sensitivity of the system is below $3\mu\varepsilon$. The strain sensing coefficients are $-0.0161\mu\varepsilon/g$ and $-0.0135\mu\varepsilon/g$ for stress increase and decrease respectively. And the error

between the practical strain value demodulated by the system and theoretical value is below 5%.

ACKNOWLEDGMENTS

This work was supported by the National Natural Science Fund of China under contact No. 60577013, and the New Century Support Program for Talented Young Teachers in Universities, MOE (Ministry of Education), China. We acknowledge the support of this work in system development and field test by Roads and Traffic Authority (RTA) and Railway Corporation (RailCorp) of NSW, Australia.

References

1. Alan D. Kersey, Michael A. Davis and Heather J. Patrick, et al, "Fiber Grating Sensors", J. Lightwave. Technol. **15(8)**, 1442-1463 (1997)
2. Y. N. Ning, A. Meldrum and W. J. Shi, et al, "Bragg grating sensing instrument using a tunable Fabry-Perot to detect wavelength variations", Meas. Sci. Technol. **9,** 599-606 (1998)
3. A. D. Kersey, T. A. Berkoff and W. W. Morey, "High resolution fiber Bragg grating based strain sensor with interferometric wavelength shift detection", Electron. Lett. **28(3)**, 236-238 (1992)
4. Serge M. Melle, Kexing Liu and Raymond M. Measures, "A Passive Wavelength Demodulation System for Guided-Wave Bragg Grating Sensors", IEEE Photonic. Tech. L. **4(5)**, 516-518 (1992)
5. Serge M. Melle, A. Tino Alavie, Shawn Karr, et al, "A Bragg Grating-Tuned Fiber Laser Strain Sensor System", IEEE Photonic. Tech. L. **5(2)**, 263-266 (1993)
6. A. D. Kersey, T. A. Berkoff and W. W. Morey, "Multiplexed fiber Bragg grating strain-sensor system with a fiber Fabry-Perot wavelength filter", Opt. Lett. **18(16)**, 1370-1372 (1993)
7. M. G. Xu, H. Geiger, J. L. Archambault, et al, "Novel interrogating system for fibre Bragg grating sensors using an acousto-optic tunable filter", Electron. Lett. **29(17)**, 1510-1511 (1993)
8. M. A. Davis and A. D. Kersey, "All-fibre Bragg grating strain-sensor demodulation technique using a wavelength division coupler", Electron. Lett. **30(1)**, 75-77 (1994)
9. M. A. Davis and A. D. Kersey, "Application of a Fiber Fourier Transform Spectrometer to the Detection of Wavelength-Encoded Signals from Bragg Grating Sensors", J. Lightwave. Technol. **13(7)**, 1289-1295 (1995)
10. A. B. Lobo Ribeiro, L. A. Ferreira, M. Tsvetkov, et al, "All-fibre interrogation technique for fiber Bragg sensors using a biconical fibre filter", Electron. Lett. **32(4)**, 382-383 (1996)
11. R. Romero, O. Frazao, P. V. S. Marques, et al, "Fibre Bragg grating interrogation technique based on a chirped grating written in an erbium-doped fibre", Meas. Sci. Technol. **14**, 1993-1997 (2003)
12. Yu-Lung Lo, Jen-Fa Huang and Po-Hsun Sung, et al, "Intensity variation effects in fiber Bragg grating sensors scanned by a tunable filter", Meas. Sci. Technol. **11**, 1456-1462 (2000)
13. M. D. Todd, G. A. Johnson and B. L. Althouse, "A novel Bragg grating sensor interrogation system utilizing a scanning filter, a Mach-Zehnder interferometer and a 3×3 coupler", Meas. Sci. Technol. **12**, 771-777 (2001)